Deformation behaviour of Kevlar® aramid fibres

S. R. Allen and E. J. Roche
Central Research and Development Department, E. I. duPont de Nemours & Company Inc., PO Box 80356, Wilmington, Delaware 19880-0356, USA
(Received 15 September 1988; accepted 16 November 1988)

A detailed analysis of Kevlar® aramid single-filament deformation is presented. Irreversible and reversible deformations are characterized via cyclic loading experiments. The non-linear elastic response is particularly studied by means of stress perturbation experiments. A shear coupling analysis is developed and fitted to the experimental data by means of a local shear modulus G. An asymptotic modulus E_a characteristic of the local orientation and an orientation angle characteristic of the large-scale misorientation are deduced. The values obtained are in agreement with those quoted in earlier structural investigations. Direct correlation between the pleated structure and the deformation behaviour is demonstrated. The opening of the pleats accounts well for the non-linearity of the elastic deformation.

(Keywords: Kevlar® aramid; fibre; deformation; pleated structure)

INTRODUCTION

The deformation of aramid fibres, particularly Kevlar® fibres, has been investigated in a number of studies covering many deformation responses. Of particular interest are studies concerning the structural response to deformation. Early on, Ballou[1] and Schaefgen *et al.*[2] concluded from sonic modulus measurements that molecular orientation improved during tensile deformation. Northolt[3–6] measured such changes directly by X-ray diffraction analysis and attributed the stress dependence of modulus to a progressive improvement of the crystalline orientation. Other studies include Ericksen's[7] creep analysis, Ii *et al.*'s[8] X-ray measurement of crystalline modulus and the spectroscopic analyses of Penn and Milanovich[9] and Zwaag *et al.*[10]. The molecular orientation response to deformation is therefore well established. In all previous studies, however, it has been interpreted in the restricted framework of classical polymer structure, i.e. as a phenomenon dealing with local orientation of crystallites. Such an interpretation ignores the prominent supramolecular organization typical of Kevlar® aramid fibres resulting from the unique liquid-crystalline processing. It was first briefly described by Ballou[1] in terms of a periodic bending of the molecular chains along the fibre direction, with the intermolecular hydrogen bonding arranged radially. Dobb *et al.*[11,12] later popularized this arrangement as a hydrogen-bonded 'pleated sheet' morphology. The simplest manifestation of this complex organization is the periodic transverse banding typical of light micrographs of the fibre (*Figure 1*), also observed from a variety of lyotropic or thermotropic polymer systems[13–20].

Other 'macroscopic' features in fibres, such as induced kink bands in Kevlar®[21,22] and undulations in poly(*p*-phenylene benzobisthiazole)[23,24] or even, on a larger scale, the zig-zag structure of collagen in rat tail tendon[25], have been shown to have a direct bearing on the tensile response. In a preliminary study[26], the authors have pointed to the relevance of the pleated structure to the deformation behaviour of Kevlar® aramid fibres. The stress dependence of modulus was shown to correspond to a progressive opening of the pleats, as measured via light scattering experiments. Additional studies are presented here to define the macrostructural response further. A thorough mechanical characterization involving cyclic experiments and analysis of time-dependent effects is discussed. The reversible pleat opening is modelled in terms of a local shearing.

EXPERIMENTAL

Single filaments taken from a 200 denier Kevlar® 29 yarn and from 1140 denier yarns of Kevlar® 49 and 149 were used for the investigations. Mechanical testing was performed using an Instron 1122 testing machine interfaced with a Hewlett–Packard series 300 computer to provide programmed deformation histories and data analysis. Generally, a 5.08 cm gauge length was employed to minimize the influence of machine compliance on the deformation response. Under these conditions the error due to machine softness amounts to a 7–10% reduction in calculated moduli values for moduli in the range of 125–190 GPa (1000–1500 g/denier). Filaments were clamped directly using flat metal grip faces. This gripping arrangement was found to provide results comparable to those obtained from fibres that were bonded with epoxy onto paper tabs. Filament size (denier) was individually measured using a Vibromat M (Textechna, Herbert Stein GmbH and Co.).

Deformation of the fibres was generally calculated from the rate of testing and elapsed time although some tests were run using a crosshead motion detector to verify accuracy. Generally, a strain rate of 10% min^{-1} was used unless otherwise noted. The data collection rate was chosen to provide incremental strain readings of roughly 0.0001. Local moduli vs. stress or strain values were obtained from linear regression of the stress–strain data using a total of 11 data pairs, five just prior to and five

0032-3861/89/060996-08$03.00

Figure 1 Optical micrograph of Kevlar® 49 fibre revealing the banded texture; fibre diameter is approximately 12 μm

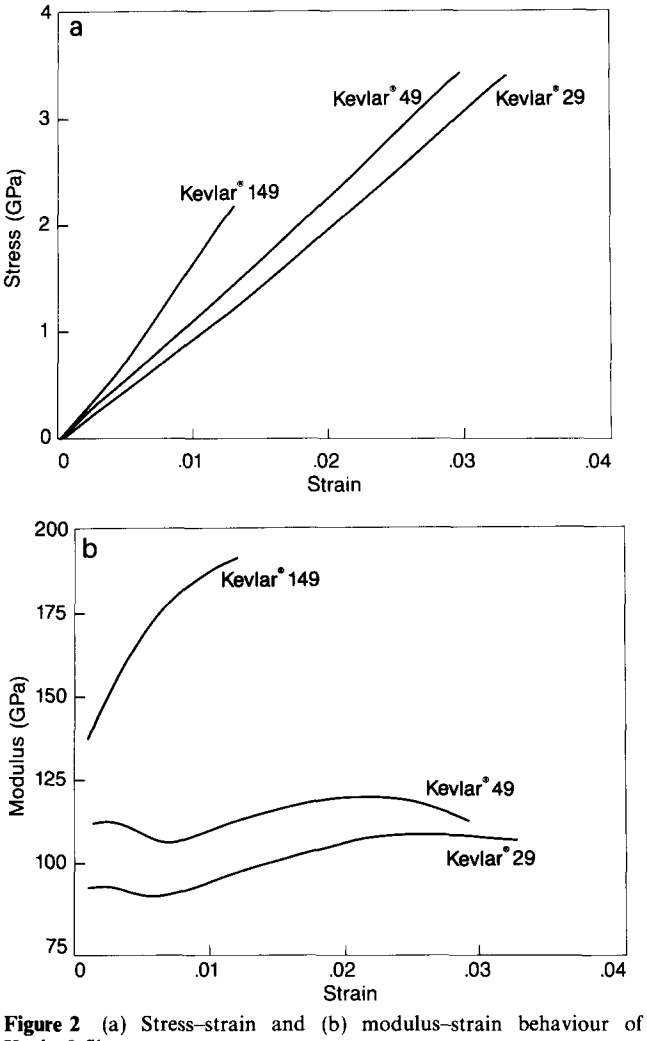

Figure 2 (a) Stress–strain and (b) modulus–strain behaviour of Kevlar® fibres

just after any point. This generally represented a local strain window of approximately 0.0011 over which local moduli were evaluated.

RESULTS

Initial loading

The tensile deformation response of Kevlar® aramid fibres is characterized by high modulus and high strength. From single extensions to break, the deformation response appears roughly linear (*Figure 2a*). The subtle non-linear character, however, is more easily observed by differentiation of the stress–strain curves to yield modulus–strain curves as shown in *Figure 2b*. For Kevlar® 29 and 49, an initial modulus can be defined in the low-strain region (e.g. 0.001–0.004) where the modulus–strain behaviour is reasonably flat. At slightly higher strains a drop in modulus is observed corresponding to a slight shoulder in the stress–strain curve at about 0.5% strain. Above 0.5% strain the modulus increases with strain and eventually levels off and may drop slightly near break. In dramatic contrast to Kevlar® 29 and 49, the higher modulus Kevlar® 149 fibres exhibit an approximately parabolic stress–strain curve where the modulus increases continually with deformation.

Cyclic loading

Associated with the tensile deformation response of aramid fibres are irreversible deformations which are more easily examined from cyclic experiments[4,6,7,28]. *Figure 3* illustrates the response of Kevlar® 49 fibres to a series of six successively increasing loads. The fibre exhibits irreversible deformation which increases with increased loadings. The magnitude of the irreversible deformation is given in *Figure 4* as a function of the maximum strain imparted to the fibre, ε_m. For maximum strains below approximately 0.5%, negligible irreversible deformation is observed. Further straining induces irreversible deformation whose magnitude increases with strain. The magnitude of the irreversible deformation is primarily determined by the maximum strain or stress that the fibre has experienced, in agreement with previous findings[4,28]. For loadings near break (3% strain) the amount of irreversible deformation approaches 0.5%. Only slight increases in irreversible deformation are found for repeated

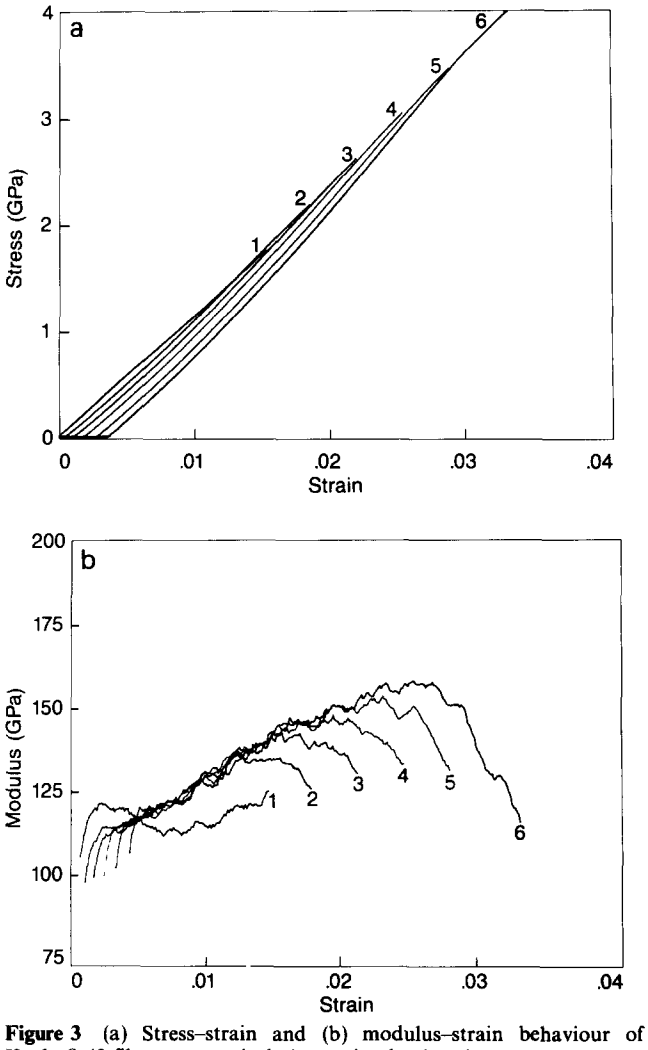

Figure 3 (a) Stress–strain and (b) modulus–strain behaviour of Kevlar® 49 fibres; successively increasing load cycles 1 to 6

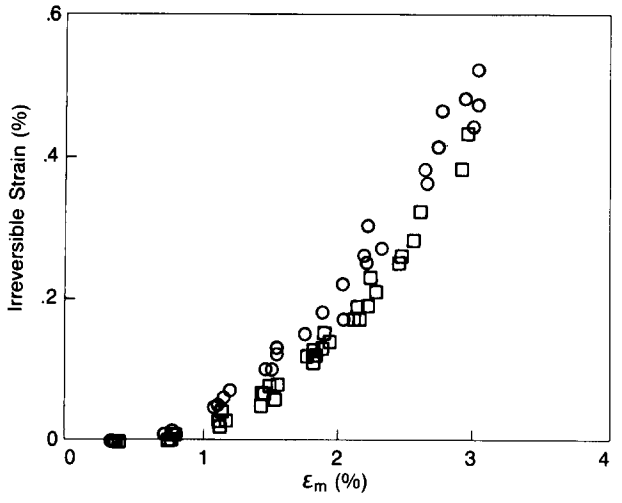

Figure 4 Irreversible deformation resulting from cyclic deformations vs. maximum cyclic strain for Kevlar® 49. Successively increasing (□) and repeated (○) loading cycles

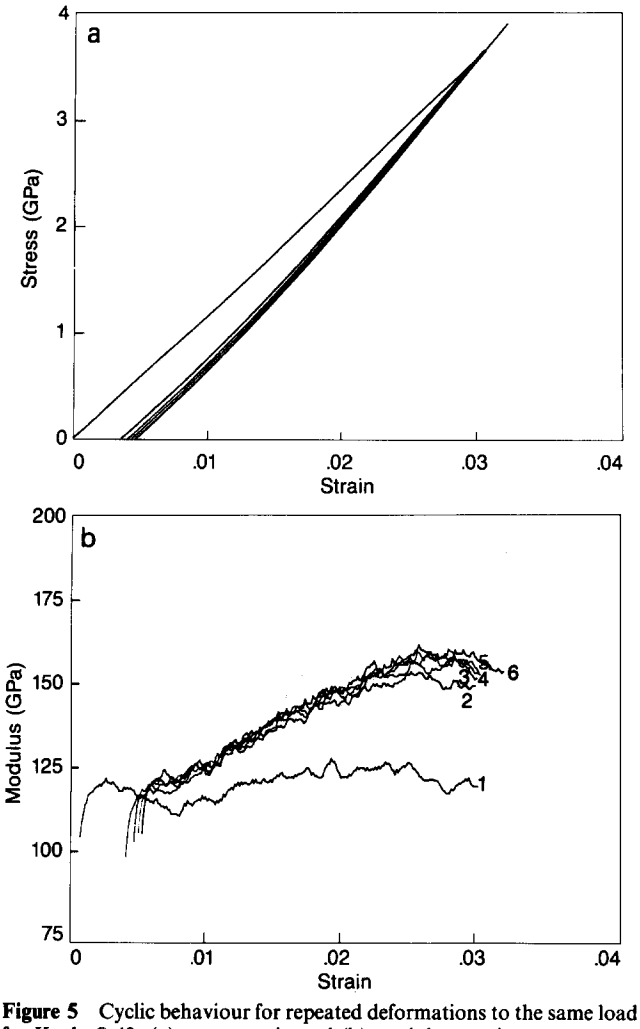

Figure 5 Cyclic behaviour for repeated deformations to the same load for Kevlar® 49: (a) stress–strain and (b) modulus–strain

loadings (*Figures 5a* and *6*) or for loadings of successively decreasing magnitude (*Figure 7a*).

The reloading response curves to successively higher load values (*Figure 3a*) are essentially parallel to one another, being offset by different amounts of irreversible deformation (determined by ε_m). When a reloading cycle is taken to values exceeding the maximum stress or strain that the fibre has experienced, the deformation response maps out the behaviour expected from single extensions to break[4] (e.g. *Figure 2*). The reloading responses shown in *Figures 3a*, *5a* and *7a* display an upward curvature with the stress–strain curves appearing almost parabolic. This non-linear loading response is more easily observed from the modulus vs. strain curves. *Figure 3b* illustrates the modulus behaviour observed from the series of loading cycles of *Figure 3a*. During the first loading cycle the modulus–strain behaviour is as observed from single extensions to break (e.g. *Figure 2b*). Subsequent loading

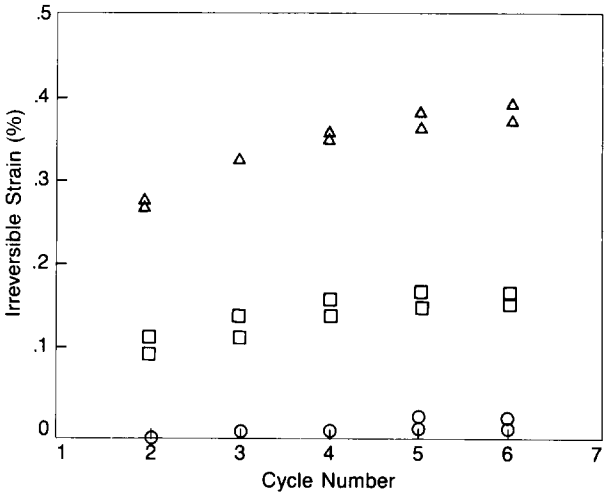

Figure 6 Irreversible deformations observed for repeated loading cycles, for Kevlar® 49: (○) 0.8 GPa, (□) 1.7 GPa, (△) 3.2 GPa

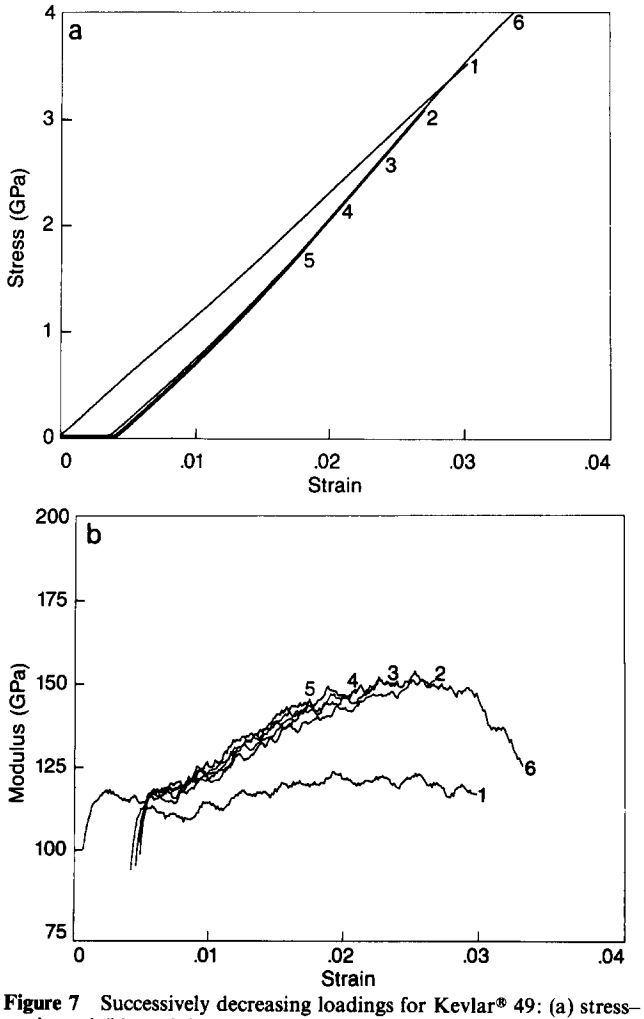

Figure 7 Successively decreasing loadings for Kevlar® 49: (a) stress–strain and (b) modulus–strain

curves, however, show an almost linear increase of local modulus with strain for strains less than ε_m, consistent with the parabolic appearance of the stress–strain curves. Additional irreversible deformation is induced as the strain exceeds ε_m giving rise to a drop in modulus and a rejoining of the modulus–strain curve observed for single extensions to break. The parallelism of the reloading stress–strain curves is confirmed by the overlap of the modulus–strain curves prior to exceeding ε_m in any loading cycle.

For repeated loading cycles up to ε_m, the modulus–strain behaviour, like the stress–strain behaviour, is practically identical (*Figures 5b* and *7b*). The underlying elastic deformation behaviour of the fibres is most closely revealed in the case where loadings are taken to near the anticipated break point. During the early loading response the modulus increases roughly linearly with deformation (*Figure 5b*) until at high deformations (>2%) the modulus–strain behaviour flattens out and the stress–strain response appears more closely linear (*Figure 5a*). Thus, the underlying elastic deformation response of the fibre is initially non-linear.

Similar non-linear behaviour was also found for Kevlar® 29 fibres examined in cyclic tests with slightly larger irreversible deformations being observed. Irreversible deformations are minimal for the Kevlar® 149 fibres and the non-linear response seen in simple tensile tests is also found in cyclic work.

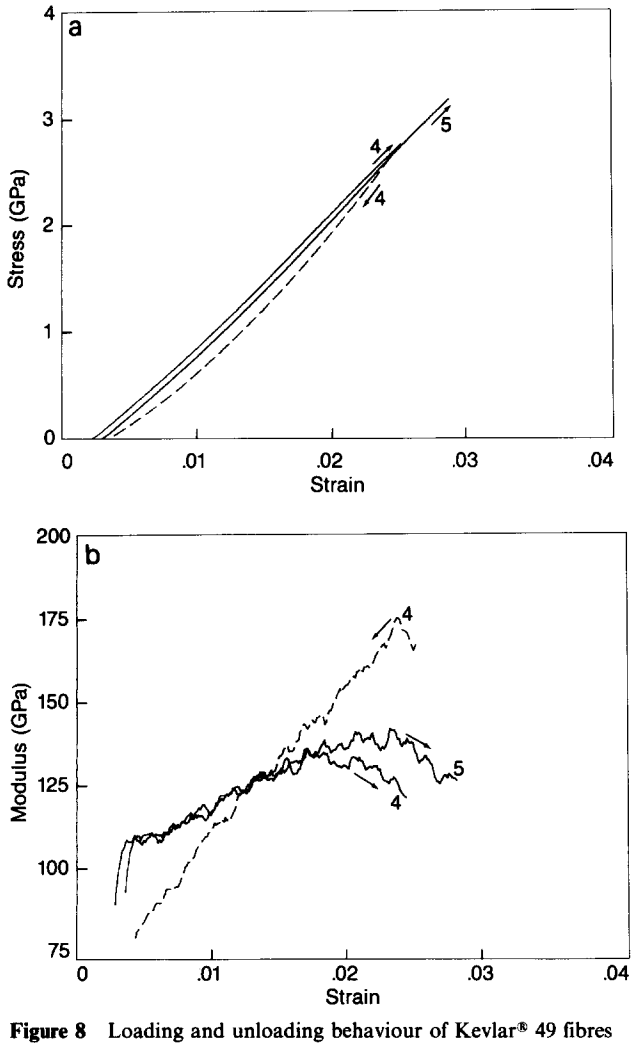

Figure 8 Loading and unloading behaviour of Kevlar® 49 fibres

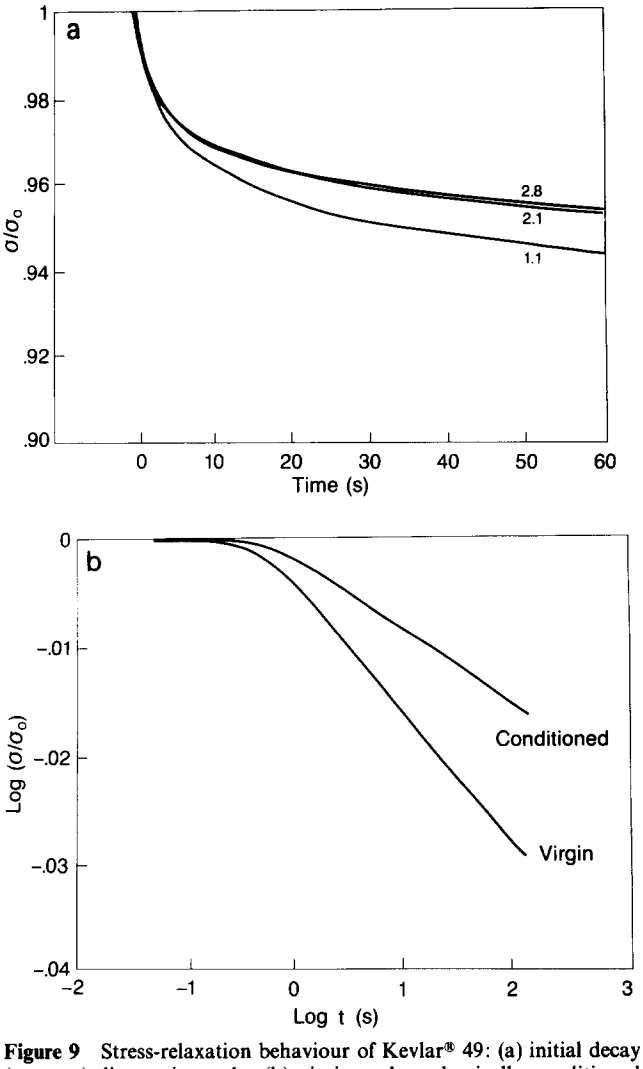

Figure 9 Stress-relaxation behaviour of Kevlar® 49: (a) initial decay (see text), linear timescale; (b) virgin and mechanically conditioned fibre relaxation responses

Time dependence

The unloading response curves from any loading cycle are not identical to their corresponding loading or subsequent reloading curves. *Figure 8* illustrates the differences between loading and unloading for both the stress–strain and modulus–strain curves for cycles taken from a successively increasing load history. The stress response displays a slight time-dependent character which is more apparent in the modulus response. This time-dependent behaviour is consistent with the magnitude of the stress relaxation observed in simple stress-relaxation tests.

Figure 9a illustrates typical stress-relaxation responses for Kevlar® 49 fibres using a linear timescale for initial stress loadings of approximately 1.1, 2.1 and 2.8 GPa. Most of the relaxation occurs over the first 5–15 s, with a slower decay over longer periods of time. The overall relaxation behaviour in aramid fibres has previously been represented by power-law models[4,7,29]. The relative amount and rate of stress relaxation is greater in virgin fibres than that observed after mechanical conditioning to high loads[7] (*Figure 9b*). The short timescale relaxation response is sufficient to cause the differences observed in *Figure 8*. Similar loading–unloading differences were found for deformation rates of 0.1, 1 and 10% min^{-1}.

Initial modulus

Figure 10 summarizes the initial modulus data for Kevlar® 49 fibres subjected to a variety of deformation histories. While permanent irreversible deformation is observed as a result of loading to high deformations, there is little change in the initial value of the subsequent reloading modulus. Thus, there is little change in the overall orientation of the fibres as a result of the irreversible deformation arising from high stress loading. Northolt[4] previously reported measurable differences in orientation between virgin poly(*p*-phenylene terephthalamide) fibres and those subjected to high loadings. These fibres, however, had much lower initial modulus than the present fibres. For the latter fibres, any differences in initial loading modulus resulting from cyclic loadings are small when compared to the changes occurring during deformation.

Elastic behaviour: perturbation tests

The non-linear deformation response is only partially observed from single extensions to break. *Figure 2* indicates a gradual increase in modulus with strain after an initial drop at 0.5%. The apparent modulus increase with deformation is suppressed in this case due to relaxations, especially that associated with the onset of irreversible deformations. Ericksen[7] has previously shown from creep experiments how the time-dependent character is reduced for mechanically conditioned fibres. The simple stress-relaxation responses (*Figure 9b*) illustrated these differences. With the extent of irreversible deformation being determined primarily by the maximum loading history, the deformation response to subsequent loadings more clearly reveals the non-linear behaviour. Tensile deformations of such 'mechanically conditioned' fibres reveal an almost parabolic appearance of the stress–strain curve. In order to evaluate the underlying elastic response, while accounting for the ongoing relaxations, we have chosen a small perturbation deformation following a relaxation in a manner similar to that employed in non-linear viscoelastic studies[30,31].

Moduli values were obtained from two types of deformation responses. For both tests a fibre sample was initially deformed at constant rate to a selected load level. At this point the crosshead was stopped and stress relaxation allowed to occur. The fibre was then deformed at constant rate to either a higher load (loading perturbation) or to a lower load (unloading perturbation). Using these procedures a number of such perturbations could be performed on a given sample. Typically a period of 30 s was found suitable to permit the majority of the stress relaxation to occur (e.g. *Figure 9a*). Longer times gave comparable results from the subsequent perturbations while much shorter times yielded results more in line with constant-rate-of-deformation results.

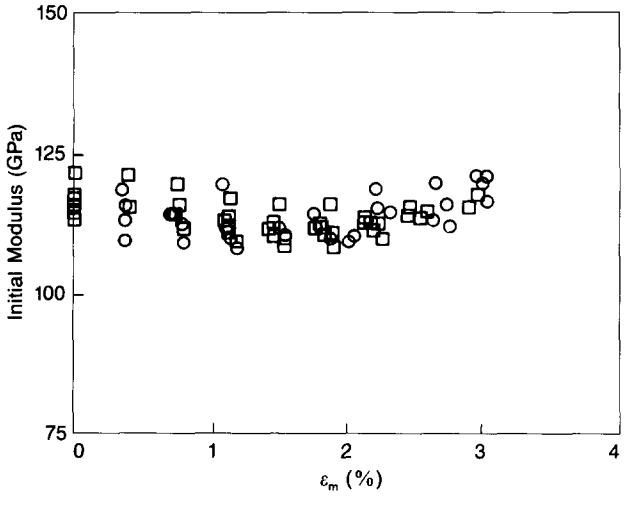

Figure 10 Kevlar® 49 initial tensile modulus after cyclic deformations. Successively increasing (□) and repeated (○) loading cycles

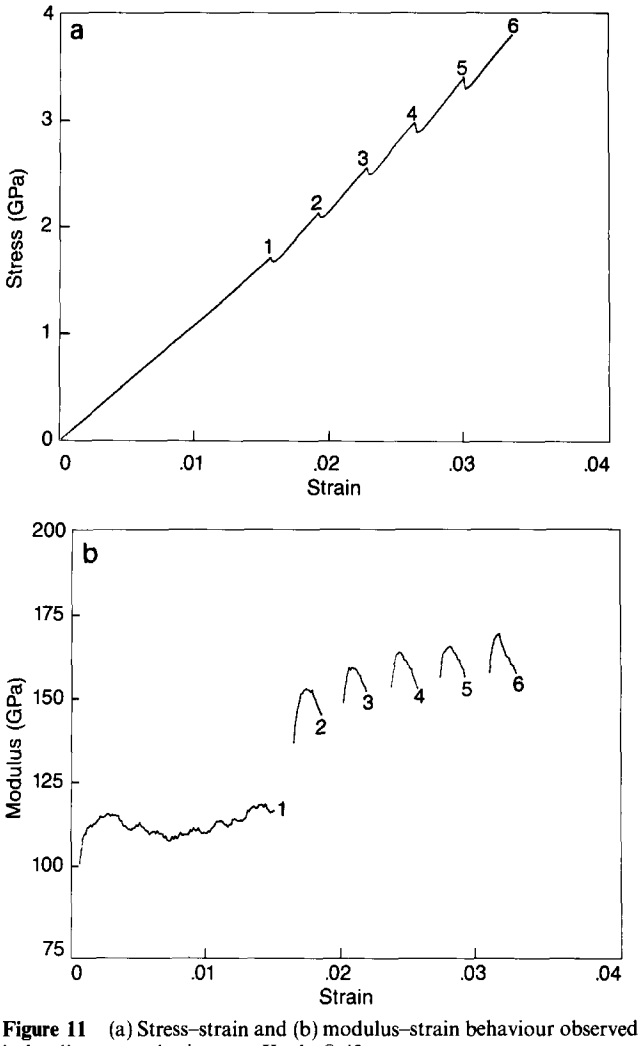

Figure 11 (a) Stress–strain and (b) modulus–strain behaviour observed in loading perturbations on Kevlar® 49

Typical behaviour observed from a series of loading perturbations is shown in *Figure 11* for Kevlar® 49. The maximum modulus value calculated during the perturbation along with the corresponding stress and strain are recorded. Moduli values obtained in this way fall between the values obtained from constant rate of loading and unloading (e.g. *Figure 8*) and provide a measure less influenced by time effects. When moduli values are compared at equivalent stress levels, good agreement is obtained between virgin and mechanically conditioned fibres, whether the values were obtained from a loading or an unloading perturbation. Good agreement is also found between the moduli values reported here and sonic moduli values obtained from similar loading studies[2,29].

DISCUSSION

Shear coupling interpretation

Aspects of the non-linear deformation response and corresponding orientation improvement which occurs during deformation of aramid fibres have been previously

described[4–6]. Various derivations have been employed, resulting in similar descriptions for the behaviour in terms of a local shearing mechanism. For completeness, we present an alternative and perhaps more general derivation here in order to account for the *supramolecular* structure of Kevlar®.

The cooperative periodic variation in orientation along the fibre axis (pleating) may be considered to respond under axial load via a local shearing. This form of coupling is similar to that observed in the non-linear elastic response of flexible fibre composites[32] and in combined torsion–tension testing of anisotropic fibres[33]. Using contracted engineering notation this coupling between an axial loading and a local shearing may be addressed by employing the generalized Hooke's law and the transformation rules to account for misorientation with respect to the axial direction. The relevant coupling between an axial loading and a shearing deformation may be described by the coupling compliance a'_{16} (ref. 33):

$$a'_{16} = (2a_{22} - 2a_{12} - a_{66}) \sin^3\theta \cos\theta - (2a_{11} - 2a_{12} - a_{66}) \cos^3\theta \sin\theta \quad (1)$$

where a_{11}, a_{22}, a_{12} and a_{66} are the *local* orthotropic compliances referred to principle directions and θ is the angle describing the local misorientation with respect to the fibre axis. The relevant components of the generalized Hooke's law will be considered in differential form:

$$\begin{aligned} d\varepsilon &= a'_{11}\, d\sigma \\ d\gamma &= a'_{16}\, d\sigma \end{aligned} \quad (2)$$

Here ε and σ are the axial strain and stress, γ the shear, and a'_{11} and a'_{16} the compliances accounting for the local misorientation (θ). The possible existence of radial and hoop stresses is ignored in that their magnitudes are expected to be small[34].

In considering only highly oriented fibres where the misorientation angles are small, the $\sin^3\theta$ term in equation (1) will be neglected. Combining equations (1) and (2) yields for the shearing:

$$d\gamma = -(2a_{11} - 2a_{12} - a_{66}) \cos^3\theta \sin\theta\, d\sigma \quad (3)$$

The local magnitude of the shearing may be approximated by the magnitude of the expected orientation change[33]. Accounting for proper sign conventions we take:

$$d\theta = -d\gamma \quad (4)$$

A description of the orientation response to loading is then obtained from equations (3) and (4) as:

$$d\theta = (2a_{11} - 2a_{12} - a_{66}) \cos^3 \sin\theta\, d\sigma$$

which upon integration yields the relationship:

$$\tan\theta = \tan\theta_0 \exp[(2a_{11} - 2a_{12} - a_{66})\sigma] \quad (5)$$

where θ_0 describes the initial misorientation in the absence of load.

The axial compliance a'_{11}, given by:

$$a'_{11} = a_{11} \cos^4\theta + (2a_{12} + a_{66}) \sin^2\theta \cos^2\theta + a_{22} \sin^4\theta$$

may be approximated as:

$$a'_{11} = a_{11} + (2a_{12} + a_{66}) \sin^2\theta \cos^2\theta \quad (6)$$

in the region of high orientation. Similarly, we make use of the geometric approximation:

$$\sin^2\theta \cos^2\theta = (\tan^2\theta)/(1 + \tan^2\theta)^2 \approx \tan^2\theta \quad (7)$$

for small angles. Combining equations (2), (5), (6) and (7) results in a definition for the axial modulus under load:

$$1/E = d\varepsilon/d\sigma = a_{11} + (2a_{12} + a_{66}) \tan^2\theta_0 \times \exp[2(2a_{11} - 2a_{12} - a_{66})\sigma]$$

where E is the fibre modulus.

A further simplification for these fibres may be introduced due to the relative magnitudes of the relevant compliances such that $(2a_{11} - 2a_{12} - a_{66}) \approx -a_{66}$ (ref. 33), leading to simplified expressions for the modulus as:

$$1/E = d\varepsilon/d\sigma = a_{11} + a_{66} \tan^2\theta_0 \exp(-2a_{66}\sigma)$$

or

$$1/E = 1/E_a + [(\tan^2\theta_0)/G] \exp(-2\sigma/G). \quad (8)$$

Equation (8) provides a relationship for the modulus variation during deformation. The parameters determining the orientational and modulus response to deformation are an initial measure of the misorientation ($\tan^2\theta_0$), a local shear compliance (a_{66}) or shear modulus (G), and an asymptotic compliance (a_{11}) or modulus (E_a). The modulus during loading is predicted to increase following an exponential relation with stress, and at sufficiently high stress would asymptotically approach the value E_a. The stress–strain equation is obtained by integration:

$$\varepsilon = a_{11}\sigma + [(\tan^2\theta_0)/2][1 - \exp(-2a_{66}\sigma)] \quad (9)$$

where the strain measure ε as employed above was defined relative to the deformation state but may be taken as the conventional engineering strain e ($\varepsilon = \ln(1 + e)$) for small deformations. Obviously the orientation parameters should be considered as local averages.

Supramolecular response

In starting from equations (1) and (2) we have implied that locally there exists a cooperative misorientation such that the coupling compliance a'_{16} is non-zero. If the misorientation locally were not cooperative, such that positive and negative misorientation angles are equally probable, then the coupling compliance would on average be equal to zero due to the odd powers of the sine function (equation (1)). Certainly, at some local scale, the orientation would be considered cooperative as dictated by the crystalline nature of the fibre. The local extent of this cooperativity will dictate the particular values of the compliances (a_{ij}) involved and the magnitude of any potential coupling. The fibrillar and microvoided character of many highly oriented fibres thus provided a possible means for such orientation improvement during deformation. The potential for elastic unwrinkling of undulating regions in carbon fibres, for example, has been discussed by Ruland[35].

The modulus response to deformation for Kevlar® 49 fibres is summarized in *Figure 12a*. The values are taken from perturbation experiments performed on a number of filaments. The full curve in the figure corresponds to equation (8). The value for E_a was taken as 175 GPa to correspond to the experimental values in the region of high stress. A value of 2 GPa was used for the shear modulus as determined in previous experiments[33]. Using these two values, an initial misorientation angle of roughly 4.5° was calculated to provide the agreement shown in *Figure 12a*. This corresponds reasonably well to misorientation angles of 4–5° reported for the periodic variation in orientation associated with the fibre's pleated supramolecular structure[1,11,12,17,18].

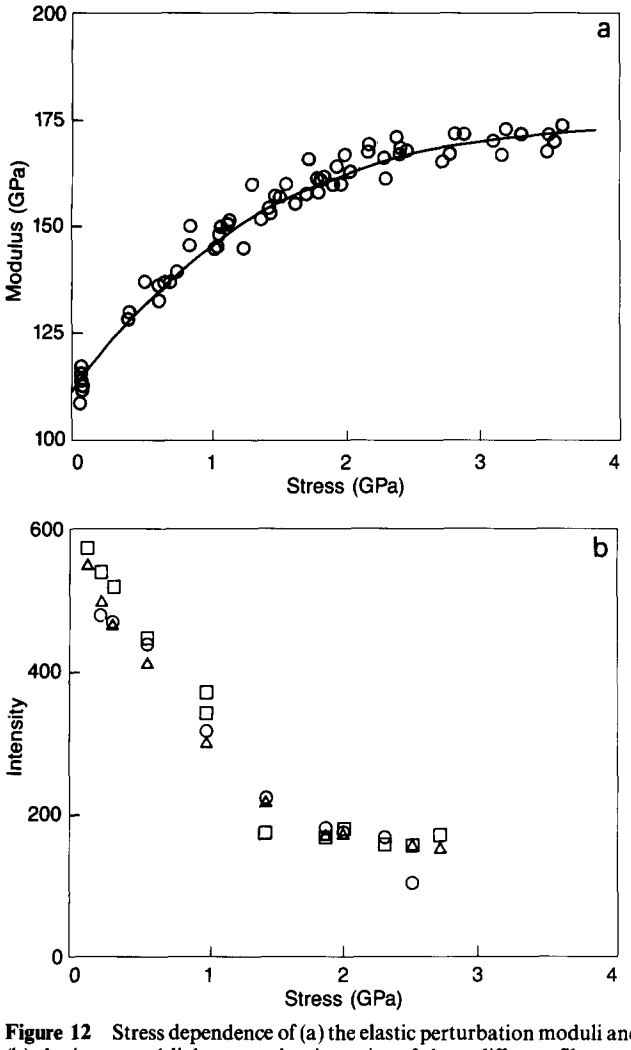

Figure 12 Stress dependence of (a) the elastic perturbation moduli and (b) the integrated light scattering intensity of three different filaments for Kevlar® 49 (the full curve in (a) corresponds to equation (8))

A comparison of the fibre's supramolecular response and mechanical response to deformation may now be made. Using light diffraction techniques, Roche *et al.*[26] have shown a correspondence between the modulus of aramid fibres and the light scattering intensity associated with the fibre's 'pleated' macrostructure. Additionally, that work demonstrated an elastic opening-up of the pleated structure in response to tensile deformation. The phenomenon is reversible, i.e. the pleats are restored upon unloading. *Figure 13* illustrates the light scattering results from this earlier work[26]. As the axial stress on the fibre is increased, there is a progressive reduction of the scattering intensity. This scattering phenomenon has been shown to result from the variation of the polarization tensor associated with the pleating[36]. The light scattering profiles in *Figure 13* have been found to vary along the length of a filament as well as between filaments. A more reproducible measure of the response to deformation was obtained from the integrated intensity under the scattering profile. *Figure 12b* summarizes the integrated intensity data, normalized to the maximum (no-load) intensity, for three different Kevlar® 49 filaments observed during static loading studies[26]. There is a pronounced decrease in scattered intensity as the stress is increased from 0 to roughly 1.7 GPa. For higher stresses the scattered intensity remains roughly constant until filament rupture.

The agreement between the modulus response to deformation and the fibre's orientational response as measured by modification of the pleated supramolecular structure is striking. Both the scattering intensity and modulus response to stress are found to be reversible during loading and unloading. Thus, the underlying non-linear elastic deformation response of Kevlar® fibres is primarily accounted for by the response of the pleated supramolecular structure of the fibres. This is a unique instance in which a molecular deformation is observed through the modification of a 'macrostructure' for a synthetic fibre. The behaviour is strikingly similar to many biological materials where the suprastructure provides for non-linear deformation responses such as in the zig-zag macrostructure of collagen in rat tail tendons[25].

A few additional comments may be made in relation to the modelling. The agreement between the misorientation values calculated via equation (8) and those measured from morphological studies favours this macrostructural approach. The value of 2 GPa for G, taken from fibre torsional studies[33], is also consistent with this analysis. The value of 175 GPa for E_a ($1/a_{11}$) is lower than a value of 220–240 GPa employed in previous analyses of aramid fibre deformation[3–6]. The higher values are obtained from extrapolations to perfect orientation, whereas the lower value used here is taken from the experimental values in the high-stress region where the modulus appears to approach an asymptote. This choice is also supported by sonic modulus measurements[2,29]. With this macrostructural viewpoint, the value E_a is not required to be that associated with a perfectly oriented structure. Rather, E_a is considered to be the modulus characteristic of the local order (on a scale smaller than the macrostructural pleating). A lower value has also been suggested by Termonia and Smith[37] even for perfectly oriented structures due to the influence of finite molecular weights.

The corresponding data for Kevlar® 29 and 149 are summarized in *Figure 14*. The results are plotted in light of equation (8). In a more rigorous analysis, shear moduli were deduced from a linear fitting of the data. Then $(\tan^2 \theta_0)/G$ is given by the slopes of the lines and the modulus E_a by the intercepts. Shear moduli of 1.8 and 1.2 GPa were thus obtained for Kevlar® 29 and 149, respectively, in good agreement with our findings from torsional studies[38]. Likewise, the calculated initial misorientation parameters are consistent with the fibre's corresponding initial moduli and pleated characters.

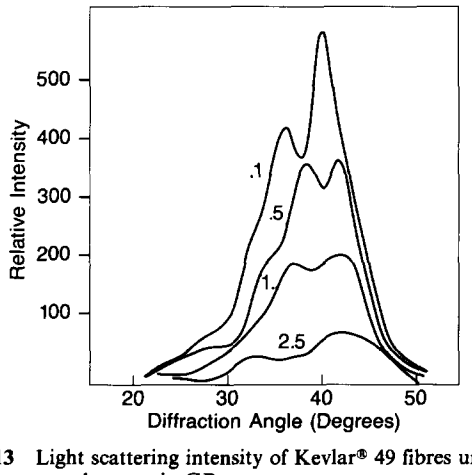

Figure 13 Light scattering intensity of Kevlar® 49 fibres under load; contour stress values are in GPa

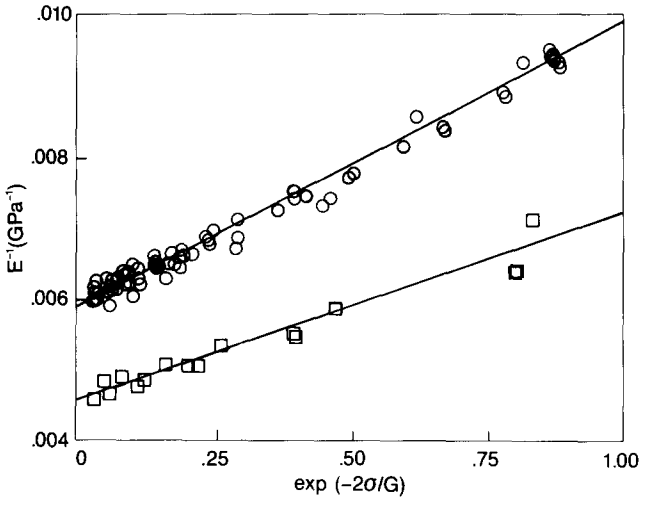

Figure 14 Moduli behaviour observed for Kevlar® 29 (○) and 149 (□); see text

Finally, the underlying elastic modulus response revealed in these studies is comparable to that observed by Ballou[1] and Schaefgen *et al.*[2] from sonic modulus measurements on yarns under load. These authors suggested that such measurements under high load provide better correlations with properties such as tenacity than do initial moduli. The single-filament techniques employed in the present investigation provide a means for similar investigations. Further studies evaluating the change in deformation response with temperature and rate of deformation would provide additional insight into the local mechanisms involved in both the elastic and irreversible deformation behaviour. The dominant influence of local shear parameters appearing in equations (8) and (9) suggests that further studies of fibre shearing behaviour, especially of time-dependent effects, are warranted.

ACKNOWLEDGEMENTS

The authors would like to thank B. Bennett and R. Molaison for experimental assistance, and Drs Y. Termonia and V. Gabara for many helpful discussions.

REFERENCES

1 Ballou, J. W. *Polym. Prep.* 1976, **17**(1) 75
2 Schaefgen, J. R., Bair, T. I., Ballou, J. W., Kwolek, S. L., Morgan, P. W., Panar, M. and Zimmerman, J. in 'Ultra High Modulus Polymers' (Eds. A. Ciferri and I. M. Ward), Applied Science, London, 1979, p. 173
3 Northolt, M. G. and van Aartsen, J. J. *J. Polym. Sci., Polym. Symp. Edn.* 1978, **58**, 283
4 Northolt, M. G. *Polymer* 1980, **21**, 1199
5 Northolt, M. G. *Br. Polym. J.* 1981, **13**, 64
6 Northolt, M. G. and v.d. Hout, R. *Polymer* 1985, **26**, 310
7 Ericksen, R. H. *Polymer* 1985, **26**, 733
8 Ii, T., Tashiro, K., Kobayashi, M. and Tadokoro, H. *Macromolecules* 1986, **19**, 1809
9 Penn, L. and Milanovich, F. *Polymer* 1979, **20**, 31
10 v.d. Zwaag, S., Northolt, M. G., Young, R. J., Robinson, I. M., Galiotis, C. and Batchelder, D. N. *Polymer* 1987, **28**, 276
11 Dobb, M. G., Johnson, D. J. and Saville, B. P. *J. Polym. Sci., Polym. Symp. Edn.* 1977, **58**, 237
12 Dobb, M. G., Johnson, D. J. and Saville, B. P. *J. Polym. Sci., Polym. Phys. Edn.* 1977, **15**, 2201
13 Donald, A. M., Viney, C. and Windle, A. H. *Polymer* 1983, **24**, 155
14 Kiss, G. and Porter, R. S. *Mol. Cryst. Liq. Cryst.* 1980, **60**, 267
15 Nishio, Y., Yamane, T. and Takahashi, T. *J. Polym. Sci., Polym. Phys. Edn.* 1985, **23**, 1053
16 Chen, S., Jin, Y., Hu, S. and Xu, M. *Polym. Commun.* 1987, **28**, 208
17 Manabe, S., Kajita, S. and Kamide, K. *Sen'i Kikai Gakkaishi* 1980, **33**, 54
18 Panar, M., Avakian, P., Blume, R. C., Gardner, K. H., Gierke, T. D. and Yang, H. H. *J. Polym. Sci., Polym. Phys. Edn.* 1983, **21**, 1955
19 Horio, M., Kaneda, T., Ishikawa, S. and Shimamura, K. *Sen-i Gakkaishi* 1984, **40**(8), T285
20 Horio, M., Ishikawa, S. and Oda, K. *J. Appl. Polym. Sci., Appl. Polym. Symp.* 1985, **41**, 269
21 DeTeresa, S. J., Allen, S. R., Farris, R. J. and Porter, R. S. *J. Mater. Sci.* 1984, **19**, 57
22 White, J. R. and Lardner, T. J. *J. Mater. Sci.* 1984, **19**, 2387
23 Allen, S. R., Filippov, A. G., Farris, R. J. and Thomas, E. L. in 'The Strength and Stiffness of Polymers' (Eds. A. E. Zachariades and R. S. Porter), Marcel Dekker, New York, 1983, p. 357
24 Allen, S. R., Farris, R. J. and Thomas, E. L. *J. Mater. Sci.* 1985, **20**, 4583
25 Diamant, J., Keller, A., Baer, E., Litt, M. and Arridge, R. G. C. *Proc. R. Soc. Lond.* (*B*) 1972, **180**, 293
26 Roche, E. J., Allen, S. R., Fincher, C. R. and Paulson, C. *Mol. Cryst. Liq. Cryst.* 1987, **153**, 547
27 VanTrump, J. E. and Lahijani, J. SAMPE Adv. Mater. Technol. '87 (Eds. R. Carson, M. Berg, K. Joller and J. J. Riel), SAMPE, 1987, p. 917
28 Bunsell, A. R. *J. Mater. Sci.* 1975, **10**, 1300
29 Schaefgen, J. R. in 'The Strength and Stiffness of Polymers' (Eds. A. E. Zachariades and R. S. Porter), Marcel Dekker, New York, 1983, p. 327
30 Sullivan, J. L. *J. Appl. Polym. Sci.* 1983, **28**, 1993
31 McKenna, G. B. and Zappas, L. J. *J. Polym. Sci., Polym. Phys. Edn.* 1985, **23**, 1647
32 Chou, T. W. and Takahashi, K. *Composites* 1987, **18**, 25
33 Allen, S. R. *Polymer* 1988, **29**, 1091
34 Allen, S. R. PhD Dissertation, University of Massachusetts, Amherst, 1983
35 Ruland, W. *J. Appl. Polym. Sci., Appl. Polym. Symp.* 1969, **9**, 293
36 Roche, E. J., Wolfe, M. S., Suna, A. and Avakian, P. *J. Macromol. Sci., Phys.* (*B*) 1985, **24**, 141
37 Termonia, Y. and Smith, P. *Polymer* 1986, **27**, 1845
38 Allen, S. R. and Roche, E. J., unpublished results